Cell. Mol. Life Sci. (2010) 67:1465–1476
DOI 10.1007/s00018-009-0255-4

Cellular and Molecular Life Sciences

RESEARCH ARTICLE

IL-13 downregulates PPAR-γ/heme oxygenase-1 via ER stress-stimulated calpain activation: aggravation of activated microglia death

Shing Hwa Liu · Cheng Ning Yang · Hung Chuan Pan · Yen Jen Sung · Ko Kaung Liao · Wen Bao Chen · Wen Zheng Lin · Meei Ling Sheu

Received: 26 October 2009 / Revised: 2 December 2009 / Accepted: 29 December 2009 / Published online: 10 March 2010

Abstract Interleukin 13 (IL-13) has been shown to induce the death of activated microglia. We observed that IL-13, but not IL-4 or IL-10, significantly enhanced endoplasmic reticulum (ER) stress induction, apoptosis and death in microglia activated by lipopolysaccharide (LPS). IL-13 enhanced ER stress-regulated calpain activation and calpain-II expression in LPS-activated microglia. Calpain-II siRNA effectively reversed the IL-13 + LPS-activated caspase-12 activation. Expression of heme oxygenase-1 (HO-1) and peroxisome proliferator-activated receptor-γ (PPAR-γ) was also increased in activated microglia, and this was effectively blocked by IL-13 and recombinant calpain. Both HO-1 inhibitor and PPAR-γ antagonist augmented, but calpain inhibitor and PPAR-γ agonists reversed, apoptosis induction in activated microglia. Transfection of PPAR-γ siRNA effectively inhibited HO-1 protein expression in activated microglia. LPS stimulated transcriptional activation of HO-1 via an increase in PPAR-γ DNA binding activity, which was reversed by IL-13. These results indicate that an ER stress-related calpain-down-regulated PPAR-γ/HO-1 pathway is involved in the IL-13-enhanced activated death of microglia.

Keywords Microglia · Interleukin-13 · Calpain · PPAR-γ · Heme oxygenase-1

S. H. Liu, C. N. Yang, and H. C. Pan contributed equally to this work.

S. H. Liu
Institute of Toxicology, College of Medicine,
National Taiwan University, Taipei, Taiwan
e-mail: shinghwaliu@ntu.edu.tw

C. N. Yang
Institute of Neuroscience, School of Life Science,
National Yang-Ming University, Taipei, Taiwan

H. C. Pan
Department of Neurosurgery, Taichung Veterans General Hospital, Taichung, Taiwan

H. C. Pan · W. B. Chen · W. Z. Lin · M. L. Sheu (✉)
Institute of Medical Technology,
National Chung Hsing University,
250 Kuo Kuang Road, Taichung 402, Taiwan
e-mail: mlsheu@nchu.edu.tw

Y. J. Sung
Institute of Anatomy and Cell Biology,
School of Life Science,
National Yang-Ming University, Taipei, Taiwan

K. K. Liao
Department of Anatomy, Chung Shan Medical University,
Taichung, Taiwan

M. L. Sheu
Department of Education and Research,
Taichung Veterans General Hospital, Taichung, Taiwan

Introduction

Inflammation in the central nervous system (CNS) is a mechanism that contributes to neuronal cell death in, for example, traumatic brain damage and stroke, and is implicated in chronic neurodegenerative diseases [1, 2]. Activated microglial cells play an important role in brain inflammatory responses. These cells normally respond to neuronal damage and remove the damaged cells by phagocytosis [3]. The activation of microglia may in turn cause neuronal damage through the release of potentially cytotoxic molecules such as cytokines, reactive oxygen species, proteinases and complement proteins [2, 4]. Moreover, previous studies have shown that interleukin 13 (IL-13), an anti-inflammatory cytokine, enhances cyclooxygenase-2 (COX-

2) expression and production of PGE2 and 15-deoxy-$\Delta^{12,14}$-PGJ2 (15d-PGJ2)] in microglia activated by lipopolysaccharide (LPS), which in turn may induce the death of activated microglia, and this may also lead to the termination of the process of brain inflammation [5, 6]. However, the molecular mechanism of the IL-13-triggered response in activated microglia still remains unclear.

Endoplasmic reticulum (ER) stress is defined as the accumulation of misfolded/unfolded proteins in the lumen of the ER [7, 8]. Neurodegenerative disorders are often characterized by the accumulation of aggregations of misfolded proteins (e.g. Alzheimer's disease, Parkinson's disease, amyotrophic lateral sclerosis) [9, 10]. ER stress has also been found to be involved in the degeneration of Purkinje cells, and activation of microglia accelerates Purkinje cell death in Purkinje cell degeneration mice [11]. Murphy and colleagues have also shown that increased macrophage colony-stimulating factor levels in Alzheimer's disease can magnify the production of β-amyloid peptide-induced microglial inflammatory cytokine and nitric oxide (NO), which in turn can intensify the cerebral inflammatory state [12]. However, it has not been elucidated whether IL-13-enhanced death of activated microglia correlates with ER stress-related signaling.

Heme oxygenase-1 (HO-1) is known to be a cytoprotective protein that is strongly induced by oxidative, nitrosative, osmotic, and hemodynamic stresses in CNS disorders [13–16]. HO-1 has also been found to stabilize the blood–spinal cord barrier and limit neutrophil infiltration through modulation of oxidative stress and white matter injury in the acutely injured spinal cord [17]. It has previously documented that HO-1 is markedly induced in activated microglia during LPS-induced brain inflammation [18]. Moreover, peroxisome proliferator-activated receptor-γ (PPAR-γ) agonists have been suggested to be potential neuroprotective agents [19–21]. HO-1 has been identified as a target gene for PPARs in vascular cells [22]. We hypothesized that depression of PPAR-γ-regulated HO-1 expression by IL-13 through the induction of ER stress-related signaling in activated microglia may exacerbate the death of microglia. The present study showed that IL-13-enhanced ER stress-related calpain activation plays an important role in the downregulation of PPAR-γ-regulated HO-1 expression in activated microglia, suggesting a potentially beneficial preventative and therapeutic strategy in brain inflammation.

Materials and methods

Chemicals and materials

LPS from *Escherichia coli* 0111:B4 prepared by phenolic extraction and gel filtration chromatography was obtained from Sigma-Aldrich. IL-13, IL-4, IL-10, and were purchased from PeproTech. The inhibitors of calpain were purchased from BIOMOL. Recombinant calpain, GW39662, 15dPGJ2, and Znpp were obtained from Merck Biosciences. GRP78, GRP94, GADD153, calpain I, calpain II, HO-1 PPAR-γ, and GAPDH were purchased from Santa Cruz Biotechnology. Antibodies agonist caspase-12, β-actin, elf2-α were obtained from Cell Signaling Technology. Lipofectin transfection reagent was purchased from Invitrogen. Specific small interfering RNA (siRNA) and scramble siRNA control were synthesized by Dharmacon (Boulder, CO, USA). Other chemicals were of the best grade available from commercial sources.

Cell culture

Microglia was cultured from the cerebral cortices of Sprague-Dawley rats aged 1–3 days as previously described [6, 23]. Briefly, the cortices were triturated into single cells in DMEM containing 10% fetal bovine serum and plated into 75 cm^2 T-flasks (0.5 hemispheres per flask) for 2 weeks. Microglia were detached from the flasks by mild shaking and applied to a nylon mesh to remove astrocytes and cell clumps. Cells were plated into 24-well plates (5×10^4 cells/well). Plates were washed 1 h later with medium to remove unattached cells. In some experiments, an immortalized microglial cells of cell line BV-2 were cultured and maintained in DMEM medium containing 10% heat-inactivated low endotoxin FBS (Life Technologies) and streptomycin/penicillin (Life Technologies) in a humidified atmosphere containing 5% CO_2.

Cell proliferation assay (MTS assay)

Cell proliferation was measured using a nonradioactive cell proliferation assay kit (CellTiter 96 AQueous; Promega, Madison, WI). The assay used a solution of tetrazolium compound [3,4-(5-dimethylthiazol-2-yl)-5-(3-carboxy-methoxyphenyl)-2-(4-sulfophenyl)-2H-tetrazolium, inner salt (MTS)] and an electron coupling reagent (phenazine methosulfate). The assay is based on the cellular conversion of the colorimetric reagent MTS into soluble formazan by dehydrogenases found only in metabolically active cells. Microglia (1×10^5/ml) in 96-well cell culture dishes were incubated for 24 h as indicated and then combined MTS/phenazine methosulfate solution was added. After 1 h of incubation at 37°C in a humidified atmosphere containing 5% CO_2, absorbance at 490 nm was measured using an enzyme-linked immunosorbent assay microplate reader. All MTS assays were repeated at least threes times in duplicate.

Transmission electron microscopy

Cells were treated with or without drugs for 18 h, and were then harvested. Cells were fixed with 4% glutaraldehyde and 2.5% paraformaldehyde dissolved in 0.1 M sodium cacodylate. Sections were prepared with a LKB Ultracut microtome (Leica, Deerfield, IL). Sections were stained with uranyl acetate and lead citrate in a LKB Ultrostainer, and examined in a JEM 1200 EX transmission electron microscope (JEOL, Peabody, MA) at an accelerating voltage of 80 kV.

Immunoblotting analysis

Protein levels were determined by Western blotting. Proteins (60 μg) were separated by SDS-PAGE, electrophoretically transferred to nitrocellulose membranes, and blocked for 1 h in phosphate-buffered saline containing Tween 20 (0.1%) and nonfat milk (5%). Blots were incubated with the HO-1, GRP78, GRP94, phospho-eIF2α, procaspase-12, GAD D153, PPAR-γ, or β-actin antibody for 1 h. Membranes were then incubated for 1 h with horseradish peroxidase-conjugated secondary antibody. After further washing with phosphate-buffered saline, blots were incubated with commercial chemoluminescence reagents (Amersham Biosciences).

HO-1 mRNA analysis

HO-1 mRNA levels were determined by Northern blotting. Total RNA (30 μg) was fractionated by electrophoresis, blot-transferred to Gene Screen Plus membranes (PerkinElmer Life Sciences), and prehybridized for 4 h at 68°C in hybridization buffer (Rapid-hyb buffer; Amersham Biosciences). Membranes were hybridized overnight at 68°C in hybridization buffer containing [^{32}P]DNA probes (1×10^8 cpm) for HO-1, glyceraldehyde-3-phosphate dehydrogenase, or 18S RNA. DNA probes were generated by RT-PCR and labeled with [α-^{32}P]dCTP using a random priming kit (Amersham Biosciences). After hybridization, membranes were washed and then exposed to X-ray film at −70°C in the presence of intensifying screens.

Electrophoretic mobility shift assay

The electrophoretic mobility shift assay was performed as described previously [24]. The consensus oligonucleotide probes were end-labeled with [γ-^{32}P]ATP according to the manufacturer's recommendations. For the binding reaction, 2 ng of the labeled oligonucleotide (approximately 20,000 cpm) and 2 μg of poly dIdC (Amersham Pharmacia Biotech) carrier were incubated with 2 μg of nuclear protein in a binding buffer (10 mM HEPES, 60 mM KCl, 1 mM DTT, 1 mM EDTA, 7% glycerol, pH 7.6) for 30 min at room temperature. Protein–DNA complexes were separated by electrophoresis on a nondenaturing 6% polyacrylamide gel and visualized by autoradiography. For competition experiments, a 100-fold excess of the unlabeled oligonucleotides was added 15 min before incubation of nuclear extracts with the end-labeled oligonucleotides.

Immunofluorescence staining

The cells were exposed for 60 min, then fixed in 4% paraformaldehyde in PBS, pH 7.4, for 15 min at 4°C, washed with PBS, blocked for 1 h at room temperature with 5% BSA in PBS, then reacted overnight at 4°C with anti-mouse monoclonal antibody (1:1,000 dilution in PBS; Santa Cruz Biotechnology). After washing, the slides were incubated for 1 h at room temperature with mouse-immunoglobulin/RPE and then viewed on a fluorescent microscope.

Calpain activity assays

Calpain activity assay was performed as described previously [24]. *N*-Succinyl-Leu-Tyr-AMC is a calpain substrate. Quantitation of 7-amino-4-methylcoumarin (AMC) fluorescence permits the monitoring of enzyme hydrolysis of the peptide–AMC conjugate and can be used to measure enzyme activity. Cells were prepared and treated on 12-well Corning/Costar plates. Prior to addition of inhibitors cells were loaded with 10 μM fluorogenic substrate (BIOMOL) and treated with LPS or IL-13 for the indicated times at 37°C in an incubator under a humidified atmosphere containing 5% CO_2. Proteolysis of the fluorescent probe was monitored using a fluorescent plate reading system (HTS-7000 Plus Series BioAssay, Perkin Elmer) with filter settings of 360±20 nm for excitation and 460±20 nm for emission.

RNA interference and transfection assays

The delivery of siRNA pools into microglia was performed using lipofectin (Invitrogen). The pooled siRNA duplexes were dissolved in buffer (20 mM KCl, 6 mM HEPES, pH 7.5, and 0.2 mM $MgCl_2$) to a concentration of 20 μM. Cell transfection was carried out for 24 h at a final siRNA concentration of 100 pM, followed by normal growth medium. Control cells were mock-transfected without siRNA, and all experimental results were confirmed using scrambled siRNA.

Annexin-V FITC and propidium iodide (PI) double staining

The annexin V/PI (BD Clontech) was used to quantify the numbers of apoptotic cells as described previously [24–26]. Cells were washed twice with PBS and stained with annexin V

and PI for 20 min at room temperature. The level of apoptosis was determined by measuring the fluorescence of the cells by flow cytometer (Becton–Dickinson). Data acquisition and analysis were performed by the CellQuest program.

Nitrite assay

Nitrite, an end-product of NO oxidation, was used as an indicator of NO production. Nitrite in conditioned medium was determined using the Griess reagent. Absorbency was determined at 550 nm using a Thermo microplate reader (Molecular Devices).

Statistical analyses

The results of this study are presented here as means±SEM. All analyses were performed by analysis of variance followed by a Fisher's least significant difference test. *P* values less than 0.05 were viewed as statistically significant.

Results

IL-13 enhances the expressions of ER stress-related markers in activated microglia

We first examined the ER stress-related unfolded protein response in activated microglia in the presence or absence of IL-13. As shown in Fig. 1, LPS increased the expressions of phospho-eIF2α, GRP94, GRP78, and GADD153 in primary and BV-2 microglial cells. IL-13 markedly enhanced the expression of these ER stress markers in activated microglia, whereas IL-13 per se had no effect on the induction of ER stress markers. Moreover, we further found that IL-13, but not IL-4 or IL-10, enhanced the phosphorylation of eIF2α in activated microglia (Fig. 1c).

To more directly assess the enhancement of IL-13 on ER stress induction in activated microglia, we examined ER morphology by transmission electron microscopy. As shown in Fig. 2, there was ER dilation in LPS-treated cells. The combination of IL-13 and LPS induced serious ER dilation with increased distention and fragmented organelles, which was consistent with the observation in microglia undergoing thapsigargin treatment (as a positive control for ER stress induction; Fig. 2e).

IL-13 enhances apoptotic cell death in activated microglia

ER stress-specific apoptosis and cytotoxicity have been shown to be involved in neurodegenerative disorders [27, 28]. We next measured cell viability and apoptosis in activated microglia. As shown in Fig. 3a, LPS significantly decreased cell viability in BV-2 microglia. IL-13 significantly enhanced, but IL-4 and IL-10 effectively reversed, the LPS-induced decrease in cell viability. In addition,

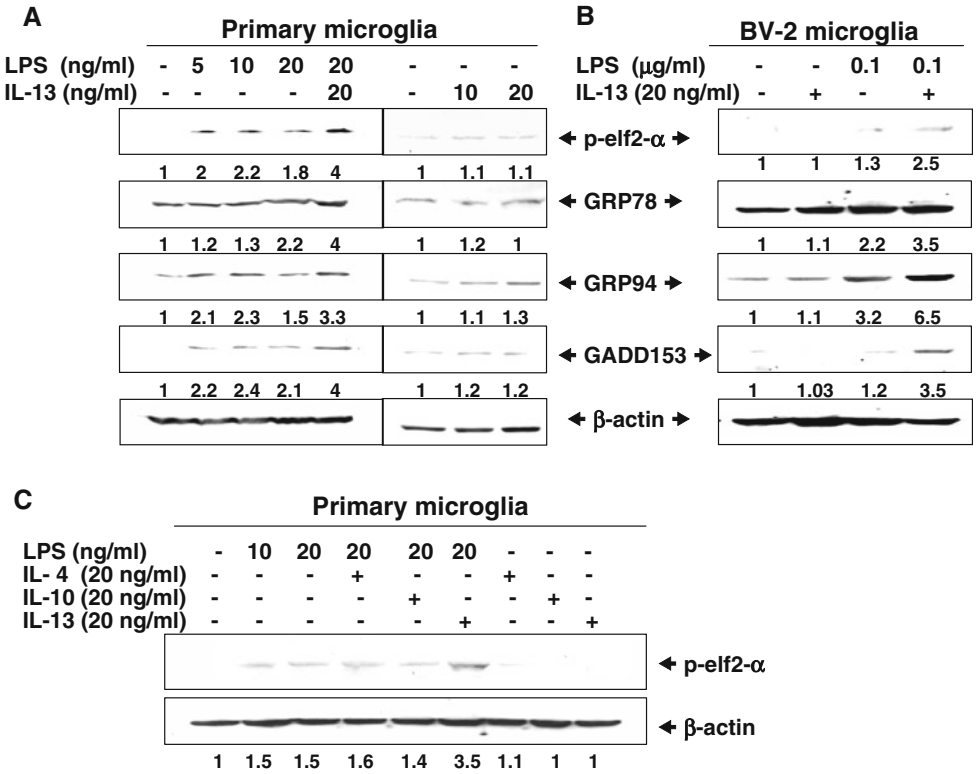

Fig. 1 IL-13 enhances ER stress markers in activated microglia. Primary microglia (**a**, **c**) and BV-2 microglia (**b**) were cultured in serum-free medium for 18 h in the presence or absence of LPS (**a** 5–20 ng/ml; **b** 0.1 μg/ml) with or without IL-13 (20 ng/ml). Cell lysates were blotted and immunostained with antibodies for phospho-eIf2-α, GRP78, GRP94 and GADD153. **c** Primary microglial cells were co-treated with LPS (10–20 ng/ml) and IL-13, IL-10, or IL-4 (20 ng/ml) for 18 h, and cell lysates were used to detect phospho-eIf2-α by Western blotting. The *numbers below* represent the fold increase in proteins relative to the untreated group after normalization to the loading control. The results shown are representative of at least four independent experiments

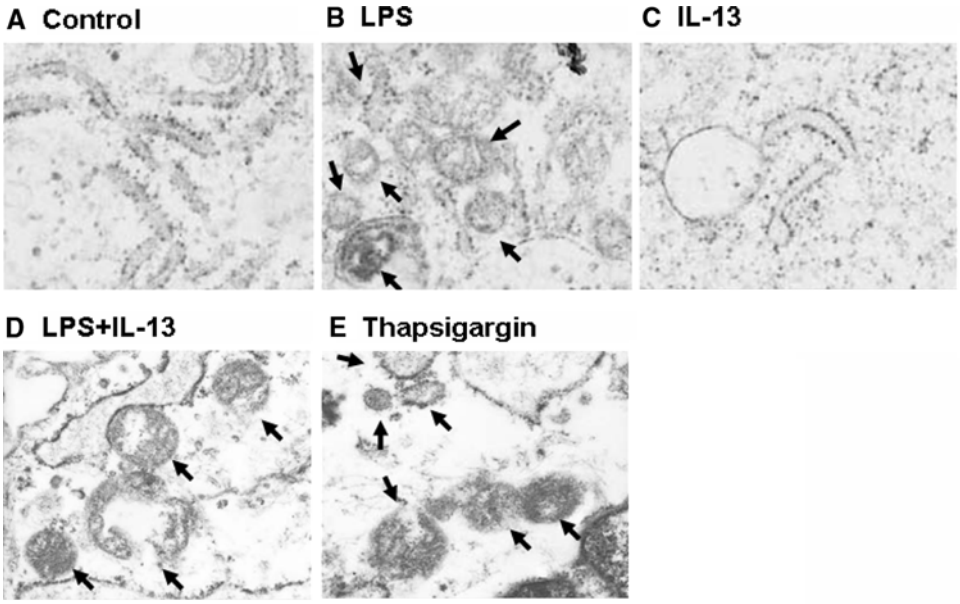

Fig. 2 IL-13 exacerbates LPS-induced ER stress examined by transmission electron microscopy. Microglial cells were treated with LPS (0.1 μg/ml) in the presence or absence of IL-13 (20 ng/ml) for 18 h. Cells were collected and visualized by electron microscopy as described in "Materials and methods". The results shown are representative of three independent experiments. **a** Control cell; **b** LPS-treated cell displays ER dilation; **c** cells treated with IL-13 alone; **d** combination of IL-13 and LPS induces serious ER dilation with increased distention and a fragmented organelle; **e** thapsigargin (1 μM) as a positive control for ER stress induction. *Arrows* indicate dilated ER. Original magnifications: ×800K

apoptosis was determined by annexin-V and PI dual staining following ER stress induction in activated microglia. As shown in Fig. 3b and c, the percentage of apoptotic cells was increased in LPS-treated microglial cells. IL-13 significantly increased apoptosis in activated microglia. Moreover, the combination of IL-13 and LPS also markedly activated caspase-12 (cleavage of pro-caspase-12) in microglia (Fig. 3d). These results indicate that IL-13 enhances apoptotic cell death in activated microglia.

Induction of calpain protein and calpain activity in activated microglia

Calpain has been demonstrated to be involved in ER stress-induced apoptotic neurodegeneration [27, 29]. We next investigated the induction of calpain activity and calpain protein expression in activated microglia. As shown in Fig. 4a and b, LPS increased the protein expression of calpain II, but not calpain I, in primary and BV-2 microglia. IL-13 (20 ng/ml) markedly enhanced calpain II protein expression in activated microglia. LPS also increased calpain activity in microglia, and this was significantly enhanced by IL-13 (Fig. 4c). Moreover, as shown in Fig. 4d, apoptosis was induced in LPS-activated microglia, and this was reversed by calpain inhibitor Z-Leu-Leu-CHO (10 μM).

We next explored the role of calpain in IL-13-enhanced ER stress-induced apoptosis in LPS-activated microglia. As shown in Fig. 5, silencing of specific calpain-II by siRNA, but not calpain-I siRNA, effectively reversed the activation of caspase-12 induced by the combination of IL-13 and LPS. These results indicate that apoptosis is induced in activated microglia by calpain-II activation under conditions of ER stress induction, and this can be enhanced by IL-13 treatment.

IL-13 inhibits LPS-induced expression of HO-1 mRNA and protein

HO-1 has been reported to be induced in activated microglia during LPS-induced brain inflammation [18]. We next investigated the effect of IL-13 on HO-1 expression in activated microglia. LPS markedly induced the expression of HO-1 mRNA (Fig. 6a) and protein (Fig. 6b) in microglia in a dose- and time-dependent manner. When the cells were pretreated with the transcription inhibitor actinomycin D or the protein synthesis inhibitor cycloheximide, expression of HO-1 mRNA and protein was decreased dramatically (Fig. 6c). IL-13 effectively inhibited the induction of HO-1 mRNA and protein expression in LPS-activated microglia (Fig. 6c and d). Moreover, the HO-1 inhibitor zinc protoporphyrin IX (Znpp) effectively enhanced LPS-induced cell apoptosis in microglia (Fig. 3c). These results indicate that HO-1 induction plays a protective role in inflammation-activated microglia.

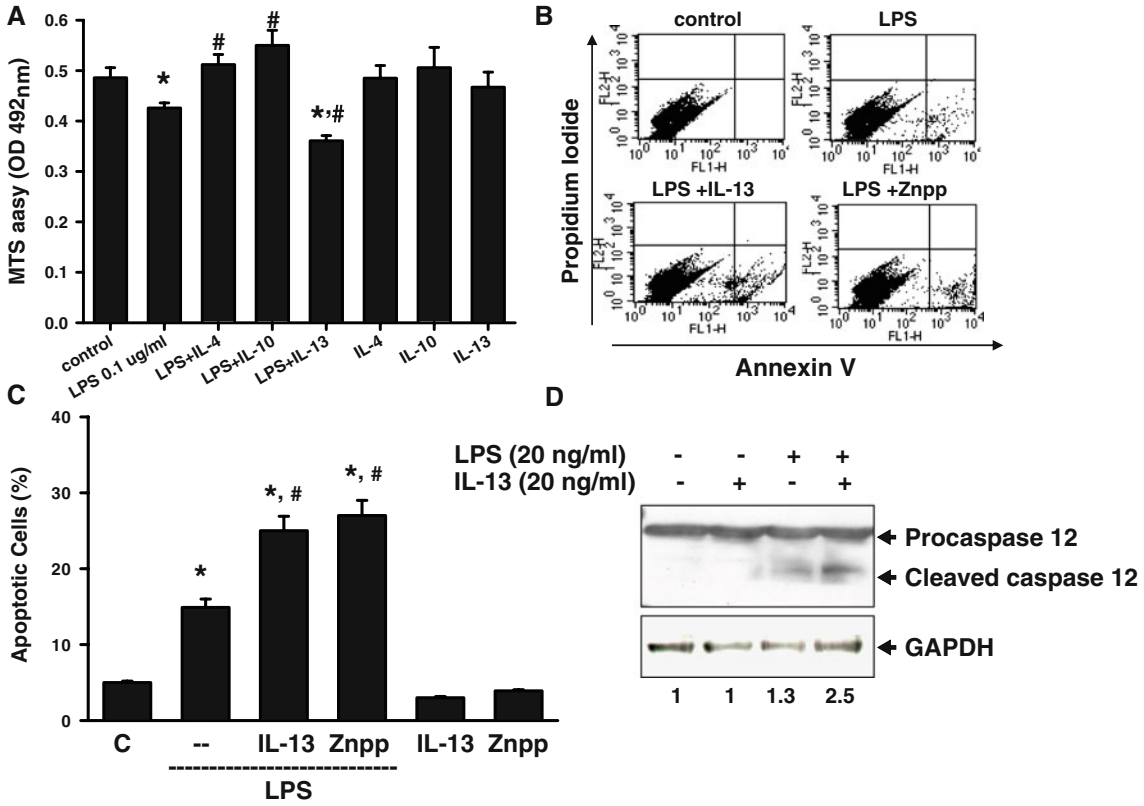

Fig. 3 IL-13 enhances apoptosis and cytotoxicity in activated microglia. BV-2 microglial cells were treated with LPS (0.1 μg/ml) in the presence or absence of IL-14, IL-10 or IL-13 (20 ng/ml) or HO-1 inhibitor ZnPP (10 μM) for 24 h. **a** Cell viability was measured. **b** Apoptosis was analyzed by annexin V/PI staining as described in "Materials and methods". **c** Apoptotic cells were quantified by densitometric analysis. Data are presented as means±SEM (n=5). *P<0.05 as compared with control; #P<0.05 as compared with LPS alone. **d** Rat primary microglia were treated with LPS (20 ng/ml) in the presence or absence of IL-13 (20 ng/ml) for 24 h. Caspase-12 cleavage was measured by Western blotting. The results shown are representative of at least three independent experiments. The *numbers below* represent the fold increase in proteins relative to the untreated group after normalization to the loading control

IL-13 inhibits LPS-induced PPAR-γ induction

PPAR-γ agonists have been suggested to be potential neuroprotective agents [20, 21]. We next investigated the role of PPAR-γ in activated microglia with or without IL-13 treatment. LPS-activated microglia showed a marked PPAR-γ nuclear translocation on analysis of immunofluorescence staining (Fig. 7a) and Western blotting (Fig. 7b). IL-13 and the PPAR-γ antagonist GW9662 effectively reversed LPS-induced PPAR-γ nuclear translocation (Fig. 7a, b). 15dPGJ$_2$, as a positive control for PPAR-γ activation, also increased PPAR-γ nuclear translocation. Moreover, LPS markedly increased PPAR-γ DNA binding activity in microglial cells, and this was effectively reversed by IL-13 (Fig. 7c). Addition of unlabeled consensus PPAR-γ oligonucleotide (100-fold excess) completely abolished the mobility shift band, demonstrating the specificity of the protein/DNA interaction (data not shown). On the other hand, preincubation of the PPAR-γ antagonist GW9662 effectively enhanced the increase in annexin V binding following treatment with LPS in microglia, while the PPAR-γ agonists 15dPGJ$_2$ and ciglitazone reversed the LPS-induced apoptosis in microglia (Fig. 7d).

We further examined the regulatory role of calpain in the expression of PPAR-γ and HO-1 and the regulatory relationship between PPAR-γ and HO-1 signals. As shown in Fig. 8, treatment of microglia with LPS resulted in an increase in the expression of PPAR-γ and HO-1 protein. IL-13 effectively decreased the expression of PPAR-γ and HO-1, while calpain inhibitor Z-Leu-Leu-CHO markedly enhanced the expression (Fig. 8a). Purified recombinant calpain II protein was also able to cleave PPAR-γ protein in the presence of $CaCl_2$ (Fig. 8b). Moreover, transfection of siRNA targeting PPAR-γ in activated microglia led to a significant reduction in HO-1 protein expression (Fig. 8b). These results imply that the calpain-downregulated PPAR-γ-regulated HO-1 signaling pathway is involved in IL-13-enhanced LPS-triggered microglial death.

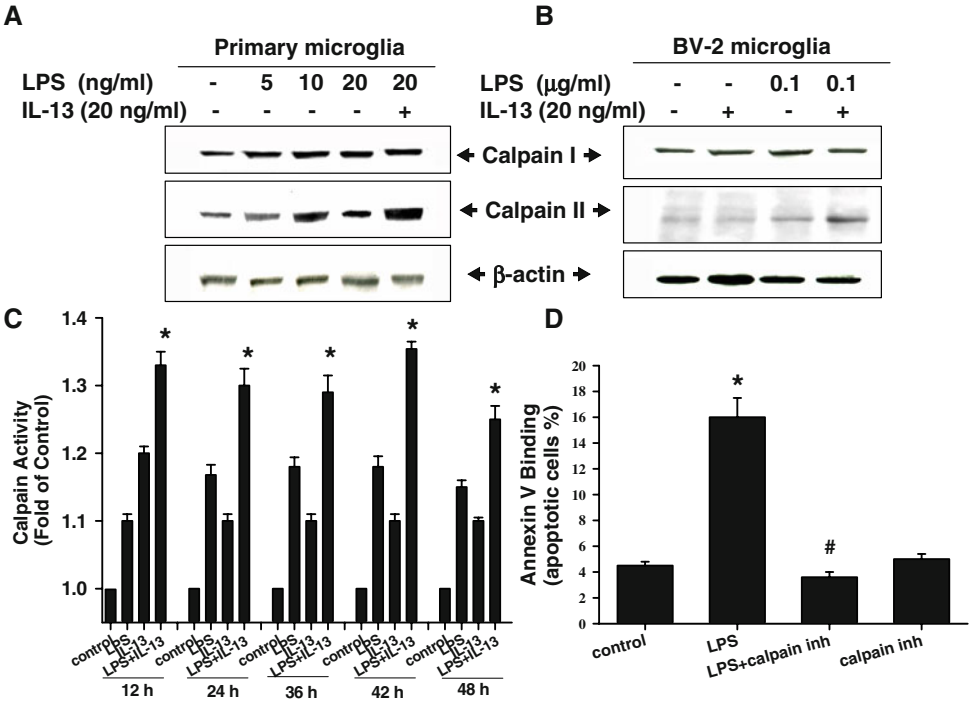

Fig. 4 Induction of calpain protein and calpain activity and apoptosis in activated microglia. Primary microglia (**a**) and BV-2 microglia (**b**) were cultured in serum-free medium for 18 h in the presence or absence of LPS (**a** 5–20 ng/ml; **b** 0.1 μg/ml) with or without IL-13 (20 ng/ml). Cell lysates were blotted and immunostained with antibodies for calpain I and II. **c** BV-2 microglia were treated with LPS (0.1 μg/ml) with or without IL-13 (20 ng/ml) for 12–48 h. Calpain activity was measured with the fluorescent calpain substrate Suc-LLVY-AMC. **d** BV-2 microglial cells were treated with LPS (0.1 μg/ml) with or without calpain inhibitor Z-Leu-Leu-CHO (10 μM) for 24 h. Apoptosis was analyzed by annexin V/PI staining. In **a** and **b**, the results shown are representative of at least four independent experiments. In **c** and **d**, data are presented as means±SEM (n=6). $^{*}P < 0.05$ as compared with control; $^{\#}P<0.05$ as compared with LPS alone

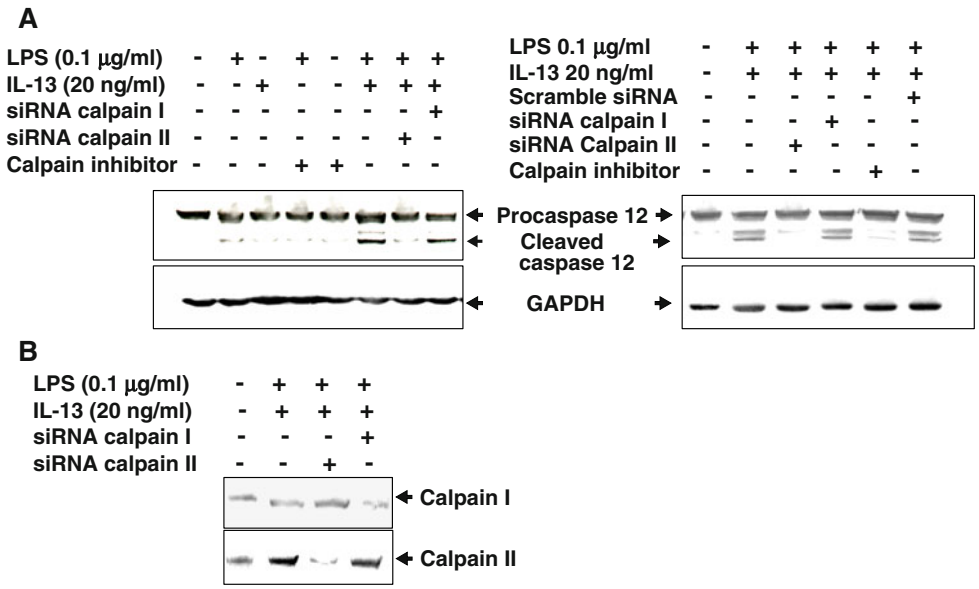

Fig. 5 IL-13 increases ER-associated caspase-12 activation in activated microglia. BV-2 microglia were cultured in serum-free medium for 18 h in the presence or absence of LPS (0.1 μg/ml) with or without IL-13 (20 ng/ml). Cells were transfected with SMARTpool siRNA duplexes (20 nM) of calpain I and calpain II. After 48 h, cells were lysed to detect caspase-12 activation (**a**, **b**) and the expression of calpain I and II proteins (**c**) by Western blotting. The effect of calpain inhibitor Z-Leu-Leu-CHO (10 μM) on caspase-12 cleavage in activated microglia was also investigated. The results shown are representative of at least three independent experiments

Discussion

Malfunction of the ER stress response can result in various diseases such as diabetes, inflammation, and neurodegenerative disorders including Alzheimer's disease, Parkinson's disease and bipolar disorder [8]. Several studies have shown that perturbation in ER calcium homeostasis plays a prominent role in the pathogenesis of

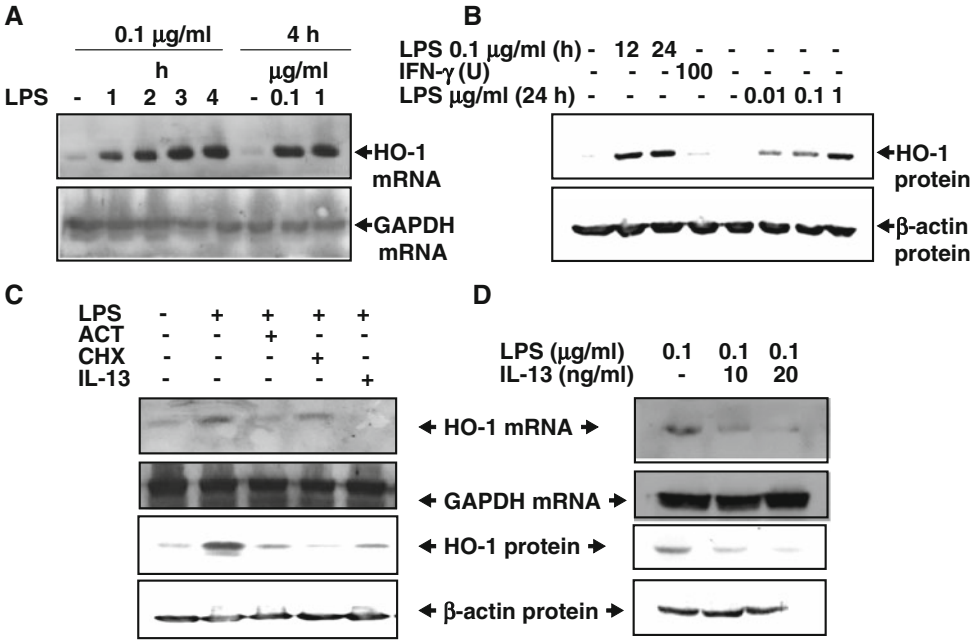

Fig. 6 IL-13 inhibits LPS-induced HO-1 mRNA and protein expression in microglial cells. BV-2 microglia were treated with LPS (0.01–1 μg/ml) in the presence or absence of cycloheximide (*CHX*, 5 μg/ml), actinomycin (*ACT*, 2 μg/ml), or IL-13 (10 and 20 ng/ml) for 1–24 h, and HO-1 mRNA and protein were determined by Northern (**a**, **c**, **d**) and Western blotting (**b**–**d**), respectively. The effect of interferon-γ (*IFN-γ*, 100 U) on HO-1 protein expression was also examined (**b**). The results shown are representative of at least four independent experiments

Alzheimer's disease [9, 30–32]. A previous study has also shown that calpain, which is activated following disruption of ER calcium homeostasis as a result of ischemic injury or amyloid-β peptide cytotoxicity, may induce apoptosis through calpain-mediated caspase-12 activation [28]. To our knowledge, the current study is the first to examine the anti-inflammatory mechanism of action of IL-13 on the process of brain inflammation through the enhancement of ER stress-triggered cell apoptosis and death in activated microglia. Our major findings are that: (1) IL-13, but not IL-4 or IL-10, augments ER stress-evoked calpain activity, which is involved in the enhancement of cell apoptosis and death in activated microglia; (2) the induction of PPAR-γ-regulated HO-1 expression plays a protective role in activated microglia; (3) IL-13 induces a downregulation of PPAR-γ-regulated HO-1 expression in activated microglia through a calpain-activated pathway.

In primary microglia, it has been reported that IL-4, IL-10, and IL-13 differentially regulate microglial responses to β-amyloid peptides and LPS, and may play a role in the observed inflammatory pathology surrounding senile plaques [33]. IL-4, IL-10, and IL-13 are crucially involved in the development of anti-inflammatory responses through their induction of T helper 2 (TH2) cells. However, Yang et al. [6] have reported that IL-13 augments COX-2 expression in activated microglia and enhances microglial death, which also leads to the termination of brain inflammation . The authors further indicated that IL-4 shares receptors with IL-13 and produces similar effects, but IL-10 and TGF-β neither enhance COX-2 expression nor induce death of activated microglia [6]. Both IL-4 and IL-13 have also been shown to induce death of activated microglia, which will prevent tissue damage caused by chronic inflammation [23]. Nevertheless, it has been suggested that IL-4 and IL-13 can induce distinct functional responses through identical type II IL-4/IL-13 receptor heterodimers [34]. LaPorte et al. [35] have also shown that this type II IL-4/IL-13 receptor heterodimer (IL-4Rα/IL-13Rα1) signals with different potencies and kinetics in response to IL-4 and IL-13. In the present work, we found that IL-13, but not IL-4 or IL-10, enhances the phosphorylation of eIF2α and cell viability in LPS-activated microglia. These findings imply that these anti-inflammatory cytokines may have opposite reactivity in response to microglial activation during brain inflammation. On the other hand, we found that IL-13, but not IL-4 or IL-10, enhances cell death in activated microglia; however, Yang et al. have shown that both IL-13 and IL-4 induce cell death in activated microglia. The major difference in experimental procedures between these two studies seems to be the source of LPS. LPS used in the study of Yang et al. was isolated from *Salmonella enteritidis*, but we used LPS from *E. coli*. Some studies have shown that *Salmonella* LPS and *E. coli* LPS may show differences in cytokine secretion [36] and cytokine-mediated lethal effect [37].

Calpain is a Ca^{2+}-activated neutral cysteine protease. There are two ubiquitous calpain isoforms: μ-calpain (calpain I, activated by micromolar concentrations of Ca^{2+}) and m-calpain (calpain II, activated by millimolar

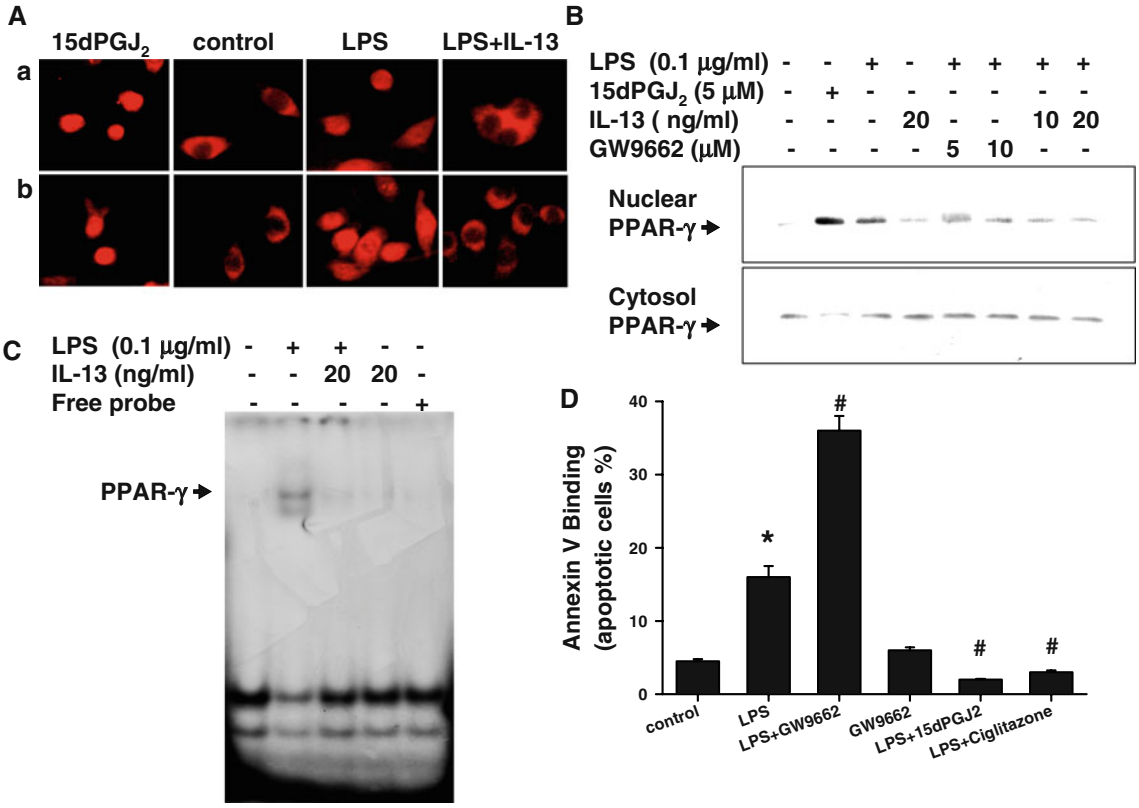

Fig. 7 IL-13 attenuates LPS-induced PPAR-γ activity. **a** Microglial cells grown on cover slips were treated with 15dPGJ2 (5 μM) and LPS (0.1 μg/ml) with or without IL-13 (20 ng/ml) for 1 h, and then fixed and incubated with monoclonal antibodies against PPAR-γ. Immunofluorescence staining for PPAR-γ was examined as described in "Materials and methods". Most of the nuclei in 15dPGJ2 or LPS-treated primary (**a**) or BV-2 (**b**) microglia were PPAR-γ staining positive. **b** BV-2 microglia were exposed to LPS with or without PPAR-γ antagonist GW9662 (10 μM) or agonist 15dPGJ2 (5 μM) for 1 h. The translocation of nuclear PPAR-γ protein was analyzed by Western blotting. **c** BV-2 microglial cells were treated with LPS (0.1 μg/ml) in the presence or absence of IL-13 (20 ng/ml) for 30 min, and nuclear PPAR-γ DNA binding activity was analyzed by an electrophoretic mobility shift assay. The results shown are representative of at least three experiments. **d** The effects of PPAR-γ antagonist GW9662 (10 μM) and agonists 15dPGJ$_2$ and ciglitazone (5 μM) on apoptosis in activated microglial cells were also investigated. Annexin V binding was determined by flow cytometry. Data are presented as means±SEM (n=5). *P<0.05 as compared with control; $^{\#}P$<0.05 as compared with LPS alone

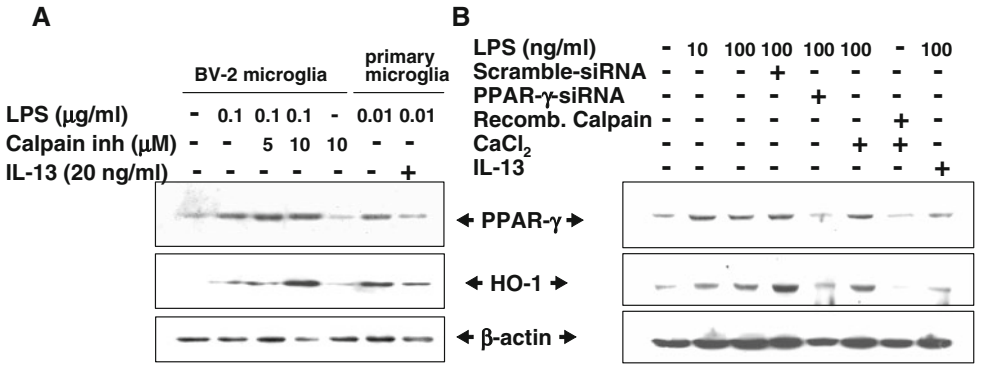

Fig. 8 The role of calpain in PPAR-γ-regulated HO-1 expression in activated microglia. Microglia were treated with LPS (0.01–0.1 μg/ml) in the presence or absence of calpain inhibitor Z-Leu-Leu-CHO (5 and 10 μM) and IL-13 (20 ng/ml) for 24 h, and the expression of PPAR-γ and HO-1 protein (**a**, **b**) was determined by Western blotting. In some experiments, BV-2 cells were transfected with siRNA-PPAR-γ or treated with purified recombinant calpain II protein plus $CaCl_2$ for 24 h in the presence or absence of LPS (10 and 100 ng/ml), and the expression of PPAR-γ and HO-1 protein was measured (**b**). The results shown are representative of at least four independent experiments

concentrations of Ca^{2+}). Calpain has been implicated in neurodegeneration in disorders including Alzheimer's disease, Parkinson's disease, amyotrophic lateral sclerosis, spinal cord injury, experimental allergic encephalomyelitis, and multiple sclerosis [38–40]. Inhibition of calpains has been shown to prevent neuronal and behavioral deficits in an MPTP mouse model of Parkinson's disease, which indicates an important role of calpain proteolytic activity in neuronal loss in Parkinson's disease [41]. Franco et al. [42] have shown that calpain II, but not calpain I, is required for proteolysis of the cytoskeletal and focal adhesion proteins FAK, paxillin, spectrin, and talin; they further suggested that calpain II plays an important role in limiting membrane protrusions and in regulating lamellipodial dynamics at the leading edge of migrating cells. Calpain has also been demonstrated to be involved in ER stress-induced apoptotic neurodegeneration [27, 29]. In vitro biochemical and calpain inhibitor studies in glial cells have shown that m-calpain (calpain II) is responsible for the cleavage of caspase-12 during ER stress, which mediates an ER-specific apoptosis pathway and may contribute to amyloid-β neurotoxicity [28]. Tan et al. [43] have also shown that calpain deficiency caused by genetic disruption of the calpain-related capn4 gene correlates with resistance to ER stress-induced apoptosis in embryonic fibroblasts, indicating a role for calpain in ER stress-induced apoptosis. In the present work, we found that IL-13 enhances ER stress, cleavage of caspase-12, and apoptotic cell death in LPS-activated microglia. IL-13 also induced calpain protein and activity in activated microglia. The calpain inhibitor Z-Leu-Leu-CHO effectively reversed apoptosis in activated microglia. Calpain-II siRNA, but not calpain-I siRNA, effectively reversed activation of caspase-12 enhanced by IL-13 in activated microglia. These results provide evidence that calpain activation-triggered apoptosis is induced in activated microglia under ER stress induction, which can be enhanced by IL-13 treatment.

HO-1 is a phase 2 enzyme, which is upregulated in response to electrophilic xenobiotics, oxidative stress, cellular injury and disease. The upregulated HO-1 expression helps mediate the resolution of neuroinflammation and brain disorders [44]. A recent study has shown that animals treated with sulforaphane, which elicits an antioxidant response mediated by Nrf2, display a two- to threefold increase in HO-1, a reduced abundance of microglial cells in the hippocampus and an attenuated production of inflammation markers (inducible NO synthase, IL-6, and TNF-α) in response to LPS [18]. It has also been found that there is a significantly greater degradation of myelin basic protein, an indicator of white matter damage, in HO-1-deficient mice with spinal cord injury, indicating that HO-1 modulates oxidative stress and white matter injury in an acutely injured spinal cord [17]. However, intracerebral hemorrhage-induced early brain injury and neurological deficits have been found to be reduced in HO-1 knockout mice, implying that HO-1 induction exacerbates intracerebral hemorrhage-induced early brain injury [45]. ER stress has been shown to be an inducer of HO-1 gene expression in several cell types and HO-1 acts in an autocrine fashion to inhibit cell apoptosis [46, 47]. On the other hand, PPAR-γ plays a role in regulating a myriad of biological processes in virtually all brain cell types. PPAR-γ agonist-induced neuroprotection has been shown in the chronic mouse model of Parkinson's disease and Alzheimer's disease, indicating that PPAR-γ agonists may possess therapeutic potential in inflammatory brain diseases [20, 21, 48–51]. It has been demonstrated that HO-1 expression is transcriptionally regulated by PPAR-α and PPAR-γ in vascular cells [22]. Recently, the PPAR-γ agonist rosiglitazone has been shown to enhance antioxidative activity of superoxide dismutase and glutathione, and to decrease expression of HO-1 in the hippocampus of epileptic rats [52]. It has also been found that 15d-PGJ2 and rosiglitazone at low concentrations suppress H_2O_2-induced rat and human neuronal apoptosis and necrosis and induce PPAR-γ and HO-1 expression [53]. However, the regulatory relationship between PPAR-γ and HO-1 signaling in brain inflammatory processes still remains unclear. In the present study, we found that the expression of PPAR-γ and HO-1 was increased in LPS-activated microglia, and this was reversed by both IL-13 and recombinant calpain. Transfection of siRNA targeting PPAR-γ effectively inhibited HO-1 protein expression in activated microglia. Both calpain inhibitor and PPAR-γ agonists reversed, but PPAR-γ antagonist enhanced, apoptosis induction in activated microglia. Moreover, under the present experimental conditions, PPAR-γ was inhibited at higher levels of calpain activation, indicating that calpain activation may need to be above a certain threshold in order to initiate PPAR-γ activation. These findings suggest that IL-13 aggravates inflammation-induced microglia apoptosis through a calpain-downregulated PPAR-γ-regulated HO-1 signaling pathway.

In conclusion, increasing microglial activation turned out to exacerbate brain damage. The present study provides a new insight into the amelioration of chronic brain inflammation. These results indicate that an calpain-downregulated PPAR-γ-regulated HO-1 pathway associated with ER stress is involved in IL-13-enhanced apoptosis in activated microglia, and this may play a role in reducing chronic brain inflammation by enhancing apoptosis of activated microglia.

Acknowledgments This work was supported by research grants from Taichung Veterans General Hospital, Taiwan (TCVGH-977304B), and the National Science Council of Taiwan (NSC96-2320-B-040-003-MY3).

References

1. Block ML, Hong JS (2005) Microglia and inflammation-mediated neurodegeneration: multiple triggers with a common mechanism. Prog Neurobiol 76:77–98
2. Dheen ST, Kaur C, Ling EA (2007) Microglial activation and its implications in the brain diseases. Curr Med Chem 14:1189–1197
3. Minghetti L, Ajmone-Cat MA, De Berardinis MA, De SR (2005) Microglial activation in chronic neurodegenerative diseases: roles of apoptotic neurons and chronic stimulation. Brain Res Rev 48:251–256
4. Whitney NP, Eidem TM, Peng H, Huang Y, Zheng JC (2009) Inflammation mediates varying effects in neurogenesis: relevance to the pathogenesis of brain injury and neurodegenerative disorders. J Neurochem 108:1343–1359
5. Shin WH, Lee DY, Park KW, Kim SU, Yang MS, Joe EH, Jin BK (2004) Microglia expressing interleukin-13 undergo cell death and contribute to neuronal survival in vivo. Glia 46:142–152
6. Yang MS, Ji KA, Jeon SB, Jin BK, Kim SU, Jou I, Joe E (2006) Interleukin-13 enhances cyclooxygenase-2 expression in activated rat brain microglia: implications for death of activated microglia. J Immunol 177:1323–1329
7. Zhao L, Ackerman SL (2006) Endoplasmic reticulum stress in health and disease. Curr Opin Cell Biol 18:444–452
8. Yoshida H (2007) ER stress and diseases. FEBS J 274:630–658
9. Lindholm D, Wootz H, Korhonen L (2006) ER stress and neurodegenerative diseases. Cell Death Differ 13:385–392
10. Culmsee C, Landshamer S (2006) Molecular insights into mechanisms of the cell death program: role in the progression of neurodegenerative disorders. Curr Alzheimer Res 3:269–283
11. Kyuhou S, Kato N, Gemba H (2006) Emergence of endoplasmic reticulum stress and activated microglia in Purkinje cell degeneration mice. Neurosci Lett 396:91–96
12. Murphy GM Jr, Yang L, Cordell B (1998) Macrophage colony-stimulating factor augments beta-amyloid-induced interleukin-1, interleukin-6, and nitric oxide production by microglial cells. J Biol Chem 273:20967–20971
13. Markesbery WR (1997) Oxidative stress hypothesis in Alzheimer's disease. Free Radic Biol Med 23:134–147
14. Schipper HM (2000) Heme oxygenase-1: role in brain aging and neurodegeneration. Exp Gerontol 35:821–830
15. Takeda A, Itoyama Y, Kimpara T, Zhu X, Avila J, Dwyer BE, Perry G, Smith MA (2004) Heme catabolism and heme oxygenase in neurodegenerative disease. Antioxid Redox Signal 6:888–894
16. Schipper HM (2004) Heme oxygenase expression in human central nervous system disorders. Free Radic Biol Med 37:1995–2011
17. Lin Y, Vreman HJ, Wong RJ, Tjoa T, Yamauchi T, Noble-Haeusslein LJ (2007) Heme oxygenase-1 stabilizes the blood-spinal cord barrier and limits oxidative stress and white matter damage in the acutely injured murine spinal cord. J Cereb Blood Flow Metab 27:1010–1021
18. Innamorato NG, Rojo AI, Garcia-Yague AJ, Yamamoto M, de Ceballos ML, Cuadrado A (2008) The transcription factor Nrf2 is a therapeutic target against brain inflammation. J Immunol 181:680–689
19. Kielian T, Syed MM, Liu S, Phulwani NK, Phillips N, Wagoner G, Drew PD, Esen N (2008) The synthetic peroxisome proliferator-activated receptor-gamma agonist ciglitazone attenuates neuroinflammation and accelerates encapsulation in bacterial brain abscesses. J Immunol 180:5004–5016
20. Lee SR, Kim HY, Hong JS, Baek WK, Park JW (2009) PPAR-gamma agonist pioglitazone reduces matrix metalloproteinase-9 activity and neuronal damage after focal cerebral ischemia. Biochem Biophys Res Commun 380:17–21
21. Sobrado M, Pereira MP, Ballesteros I, Hurtado O, Fernandez-Lopez D, Pradillo JM, Caso JR, Vivancos J, Nombela F, Serena J, Lizasoain I, Moro MA (2009) Synthesis of lipoxin A4 by 5-lipoxygenase mediates PPARgamma-dependent, neuroprotective effects of rosiglitazone in experimental stroke. J Neurosci 29:3875–3884
22. Kronke G, Kadl A, Ikonomu E, Bluml S, Furnkranz A, Sarembock IJ, Bochkov VN, Exner M, Binder BR, Leitinger N (2007) Expression of heme oxygenase-1 in human vascular cells is regulated by peroxisome proliferator-activated receptors. Arterioscler Thromb Vasc Biol 27:1276–1282
23. Yang MS, Park EJ, Sohn S, Kwon HJ, Shin WH, Pyo HK, Jin B, Choi KS, Jou I, Joe EH (2002) Interleukin-13 and -4 induce death of activated microglia. Glia 38:273–280
24. Sheu ML, Ho FM, Chao KF, Kuo ML, Liu SH (2004) Activation of phosphoinositide 3-kinase in response to high glucose leads to regulation of reactive oxygen species-related nuclear factor-kappaB activation and cyclooxygenase-2 expression in mesangial cells. Mol Pharmacol 66:187–196
25. Sheu ML, Ho FM, Yang RS, Chao KF, Lin WW, Lin-Shiau SY, Liu SH (2005) High glucose induces human endothelial cell apoptosis through a phosphoinositide 3-kinase-regulated cyclooxygenase-2 pathway. Arterioscler Thromb Vasc Biol 25:539–545
26. Sheu ML, Liu SH, Lan KH (2007) Honokiol induces calpain-mediated glucose-regulated protein-94 cleavage and apoptosis in human gastric cancer cells and reduces tumor growth. PLoS One 2:e1096
27. Nakagawa T, Zhu H, Morishima N, Li E, Xu J, Yankner BA, Yuan J (2000) Caspase-12 mediates endoplasmic-reticulum-specific apoptosis and cytotoxicity by amyloid-beta. Nature 403:98–103
28. Nakagawa T, Yuan J (2000) Cross-talk between two cysteine protease families. Activation of caspase-12 by calpain in apoptosis. J Cell Biol 150:887–894
29. Siman R, Flood DG, Thinakaran G, Neumar RW (2001) Endoplasmic reticulum stress-induced cysteine protease activation in cortical neurons: effect of an Alzheimer's disease-linked presenilin-1 knock-in mutation. J Biol Chem 276:44736–44743
30. Malhotra JD, Kaufman RJ (2007) Endoplasmic reticulum stress and oxidative stress: a vicious cycle or a double-edged sword? Antioxid Redox Signal 9:2277–2293
31. Uehara T (2007) Accumulation of misfolded protein through nitrosative stress linked to neurodegenerative disorders. Antioxid Redox Signal 9:597–601
32. Kim I, Xu W, Reed JC (2008) Cell death and endoplasmic reticulum stress: disease relevance and therapeutic opportunities. Nat Rev Drug Discov 7:1013–1030
33. Szczepanik AM, Funes S, Petko W, Ringheim GE (2001) IL-4, IL-10 and IL-13 modulate A beta(1–42)-induced cytokine and chemokine production in primary murine microglia and a human monocyte cell line. J Neuroimmunol 113:49–62
34. Kelly-Welch AE, Hanson EM, Boothby MR, Keegan AD (2003) Interleukin-4 and interleukin-13 signaling connections maps. Science 300:1527–1528
35. LaPorte SL, Juo ZS, Vaclavikova J, Colf LA, Qi X, Heller NM, Keegan AD, Garcia KC (2008) Molecular and structural basis of cytokine receptor pleiotropy in the interleukin-4/13 system. Cell 132:259–272

36. Habicht GS, Katona LI, Benach JL (1991) Cytokines and the pathogenesis of neuroborreliosis: borrelia burgdorferi induces glioma cells to secrete interleukin-6. J Infect Dis 164:568–574
37. Netea MG, Kullberg BJ, Joosten LA, Sprong T, Verschueren I, Boerman OC, Amiot F, van den Berg WB, Van der Meer JW (2001) Lethal Escherichia coli and Salmonella typhimurium endotoxemia is mediated through different pathways. Eur J Immunol 31:2529–2538
38. Nakanishi H (2003) Microglial functions and proteases. Mol Neurobiol 27:163–176
39. Ray SK, Banik NL (2003) Calpain and its involvement in the pathophysiology of CNS injuries and diseases: therapeutic potential of calpain inhibitors for prevention of neurodegeneration. Curr Drug Targets CNS Neurol Disord 2:173–189
40. Glynn P (2000) Neural development and neurodegeneration: two faces of neuropathy target esterase. Prog Neurobiol 61:61–74
41. Crocker SJ, Smith PD, Jackson-Lewis V, Lamba WR, Hayley SP, Grimm E, Callaghan SM, Slack RS, Melloni E, Przedborski S, Robertson GS, Anisman H, Merali Z, Park DS (2003) Inhibition of calpains prevents neuronal and behavioral deficits in an MPTP mouse model of Parkinson's disease. J Neurosci 23:4081–4091
42. Franco SJ, Rodgers MA, Perrin BJ, Han J, Bennin DA, Critchley DR, Huttenlocher A (2004) Calpain-mediated proteolysis of talin regulates adhesion dynamics. Nat Cell Biol 6:977–983
43. Tan Y, Dourdin N, Wu C, Veyra TD, Elce JS, Greer PA (2006) Ubiquitous calpains promote caspase-12 and JNK activation during endoplasmic reticulum stress-induced apoptosis. J Biol Chem 281:16016–16024
44. Syapin PJ (2008) Regulation of haeme oxygenase-1 for treatment of neuroinflammation and brain disorders. Br J Pharmacol 155:623–640
45. Wang J, Dore S (2007) Heme oxygenase-1 exacerbates early brain injury after intracerebral haemorrhage. Brain 130:1643–1652
46. Liu XM, Peyton KJ, Ensenat D, Wang H, Schafer AI, Alam J, Durante W (2005) Endoplasmic reticulum stress stimulates heme oxygenase-1 gene expression in vascular smooth muscle. Role in cell survival. J Biol Chem 280:872–877
47. Lee GH, Kim HK, Chae SW, Kim DS, Ha KC, Cuddy M, Kress C, Reed JC, Kim HR, Chae HJ (2007) Bax inhibitor-1 regulates endoplasmic reticulum stress-associated reactive oxygen species and heme oxygenase-1 expression. J Biol Chem 282:21618–21628
48. Rosa AO, Egea J, Martinez A, Garcia AG, Lopez MG (2008) Neuroprotective effect of the new thiadiazolidinone NP00111 against oxygen-glucose deprivation in rat hippocampal slices: implication of ERK1/2 and PPARgamma receptors. Exp Neurol 212:93–99
49. Contestabile A (2009) Benefits of caloric restriction on brain aging and related pathological states: understanding mechanisms to devise novel therapies. Curr Med Chem 16:350–361
50. Kapadia R, Yi JH, Vemuganti R (2008) Mechanisms of anti-inflammatory and neuroprotective actions of PPAR-gamma agonists. Front Biosci 13:1813–1826
51. Schintu N, Frau L, Ibba M, Caboni P, Garau A, Carboni E, Carta AR (2009) PPAR-γ-mediated neuroprotection in a chronic mouse model of Parkinson's disease. Eur J Neurosci 29:954–963
52. Yu X, Shao XG, Sun H, Li YN, Yang J, Deng YC, Huang YG (2008) Activation of cerebral peroxisome proliferator-activated receptors gamma exerts neuroprotection by inhibiting oxidative stress following pilocarpine-induced status epilepticus. Brain Res 1200:146–158
53. Lin TN, Cheung WM, Wu JS, Chen JJ, Lin H, Chen JJ, Liou JY, Shyue SK, Wu KK (2006) 15d-Prostaglandin J2 protects brain from ischemia–reperfusion injury. Arterioscler Thromb Vasc Biol 26:481–487